

RESEARCH PAPER

Investigation of Electronic and Topological Properties of Magnesium-coated Boron Fullerenes and Their Interaction with Hydrogen Molecule

Hashem Tavakoli Moghadam ¹, Mohsen Oftadeh ^{1*}, Nasrin Sohrabi ¹ and Mohammad Azami ²

¹ Payame Noor University, Tehran 19395-4697, IR Iran

² Chemistry Department, Yasouj University, Yasuj, Iran

ARTICLE INFO

Article History:

Received 19 October 2022

Accepted 27 December 2022

Published 01 January 2023

Keywords:

Boron fullerenes

Electronic properties

Hydrogen storage

Molecular descriptors

ABSTRACT

Various nanostructures have been widely investigated as alternative materials for hydrogen storage using experimental and computational techniques. In this research, adsorption, electronic, topological properties, and some molecular descriptors of magnesium-doped boron fullerenes and their interaction with H₂ for hydrogen storage are investigated using density functional theory at B3LYP/6-31G//M062X/6-31G** theoretical level. Structures of B₈₀, Mg₁₂B₈₀, Mg₂₀B₈₀ and Mg₃₀B₈₀ were optimized and their interaction with hydrogen molecule were analyzed. Results shows that charge transfer from Mg to B atoms is responsible for positive charge of Mg atoms. When hydrogen molecule approach to the system, it gets polarized and adsorbed to these boron fullerenes doped with Mg atoms. Also, it was found that Mg₁₂B₈₀ possesses the lowest energy gap (ΔE_{H-L}), lowest hardness (η), and the highest adsorption energy, which indicates the reactivity and the hydrogen storage capability of this structure to adsorb hydrogen rather than B₈₀, Mg₂₀B₈₀ and Mg₃₀B₈₀.

How to cite this article

Tavakoli Moghadam H, Oftadeh M, Sohrabi N and Azami M. Investigation of Electronic and Topological Properties of Magnesium-coated Boron Fullerenes and Their Interaction with Hydrogen Molecule. J Nanostruct, 2023; 13(1):254-265. DOI: 10.22052/JNS.2023.01.026

INTRODUCTION

Nowadays, nanomaterials have wide applications in human life, and a more accurate knowledge of their structure helps to extend their applications, because of relationship between macroscopic and microscopic properties. Various nanostructures, which are composed of carbon, boron and nitrogen, have been widely investigated as alternative materials for hydrogen storage using experimental and computational techniques [1-13]. One method to store hydrogen is using nanomaterials such as fullerenes and metal-coated nanotubes which have higher binding

energies [14-18]. Metal-coating of nanotubes increase the ability of the nanostructures to absorb hydrogen molecules [19]. Metals such as Sc and Ti, were among the first elements investigated for coating nanotubes and fullerenes [17, 18]. These metals show favorable binding interaction with hydrogen molecules in the range of 0.2 to 0.6 eV through the Kubas mechanism [20]. Dong et al. [21] demonstrated that the B₄₀ fullerene coated by 6 Ti atoms (Ti₆B₄₀) can store up to 34 H₂ molecules, corresponding to a maximum gravimetric density of 8.7 wt%. It takes 0.20-0.40 eV/H₂ to add one H₂ molecule, which

* Corresponding Author Email: m_oftadeh@pnu.ac.ir

assures reversible storage of H₂ molecules under ambient conditions. Tang, C and Xue, Z [22] found that the average hydrogen adsorption energies per H₂ for B₄₀ (Sc-nH₂)₆ (n =1-5) are in the energy range from 0.33 to 0.58 eV. Liu et al. [23] indicated that Sc₄B₃₈ systems could effectively absorb 24H₂ and have an average adsorption energy of 0.22 eV. Boron nanostructures coated with metal have been widely analyzed for hydrogen storage using density functional theory (DFT) [21, 24-29]. One of the conditions for reversible hydrogen molecule adsorption is that the adsorption energy lies between the energy of physical and chemical adsorption types (between 0.2 and 0.4 eV/H₂) [30]. Szwacki et al. [31] predicted a stable nanostructure of boron fullerene family and suggested a stable boron cage of B₈₀, in which the inclusion of metal atoms on these nanostructures often raises hydrogen storage capacity due to the strong binding energy. Zhou et al. reported the hydrogen adsorption on alkali-metal (Na, K) doped B₈₀. They found that Na₁₂B₈₀ and K₁₂B₈₀ show fairly low adsorption energies (0.07 eV/H₂ and 0.09 eV/H₂), indicating that alkali-metal is unsuitable for hydrogen storage. Calcium coated nanotubes and fullerenes are appropriate coating systems for hydrogen storage [5, 26, 28, 30, 32]. Yoon et al. demonstrated that calcium atoms can be placed on each of the 32 rings in C₆₀ and create the Ca₃₂C₆₀ structure that absorbs 92 hydrogen molecules [33]. A polarization mechanism for the adsorption of H₂ molecules has been developed by evaluation of the radial component of the electric field related to the charge redistribution [34]. In many cases, fullerene B₈₀ has been used as a calcium coatings substrate for binding of hydrogen molecule [35]. Since the Ca₃₂C₆₀ complex has been shown to achieve a high specific density, calcium-coated B₈₀ may achieve a similar or greater specific density. In addition, the larger surface area of B₈₀ compared to C₆₀ may make the calcium-coated B₈₀ complex a better material for adsorption H₂ molecules. Recently it has been showed that a calcium-coated B₈₀ fullerene, Ca₁₂B₈₀, is a promising material for hydrogen storage [24]. The Ca₁₂B₈₀ complex includes one calcium atom placed on each of the 12 pentagonal rings of B₈₀. The average binding energy of calcium in Ca₁₂B₈₀, 0.12–0.40 eV/H₂, is greater than the binding energy of bulk calcium metal, which highly reduces the probability of clustering in B₈₀ and it represents a high capacity hydrogen storage material with the required

properties.

Since calcium and magnesium-coated B₈₀ fullerenes exhibit high hydrogen storage capability, in this research, different magnesium-coated boron fullerenes were selected to investigate hydrogen binding energies and molecular descriptors which can provide a lot of information to interpret and predict the properties of the entitled systems.

COMPUTATIONAL DETAILS

All calculations for Mg, H₂, B₈₀, Mg₁₂B₈₀, Mg₂₀B₈₀, Mg₃₀B₈₀ systems and their complexes with hydrogen molecule have been carried out by using Gaussian 09 software [36] at B3LYP/6-31G//M062X/6-31G** level of theory, which has been shown as a popular level to predict binding energies of molecules [37], and vibrational harmonic frequency calculations have been done to confirm stable structures. The amount of charge transfer from magnesium atoms to boron atoms for Mg₁₂B₈₀, Mg₂₀B₈₀ and Mg₃₀B₈₀ when magnesium atoms are bind to boron pentagonal rings and boron hexagonal rings, respectively, has been calculated using Mulliken charge distribution. To determine the type of interaction of hydrogen molecule with B₈₀, Mg₁₂B₈₀, Mg₂₀B₈₀ and Mg₃₀B₈₀, critical points have been calculated by using AIM2000 software [38]. Some molecular descriptors are obtained for the entitled systems using Dragon ver. 7 (5270/3D) software [39].

RESULTS AND DISCUSSION

Fig. 1 shows optimized structures in which Mg atoms bind to the boron atoms in boron fullerene (B₈₀). According to the structure presented by Szwacki et al. [31], when Mg atoms bind to the boron fullerene, charge transfer takes place from Mg atoms to B atoms. Tables 1 to 3 include amount of charge transfers for Mg₁₂B₈₀, Mg₂₀B₈₀ and Mg₃₀B₈₀ when Mg atoms bind to boron pentagonal and boron hexagonal rings, calculated in the context of Mulliken population analysis. This charge transfers make Mg atoms to become positively-charged, that leads to interaction with boron fullerene with negative charge. The binding energies for boron fullerene doped with Mg is calculated by

$$E_b = (E_{MgB_{80}} - E_{B_{80}} - mE_{Mg})/m \quad (1)$$

where E_{MgB₈₀}, E_{B₈₀} and E_{Mg} are the total energy of B₈₀ doped with Mg, the energies of B₈₀

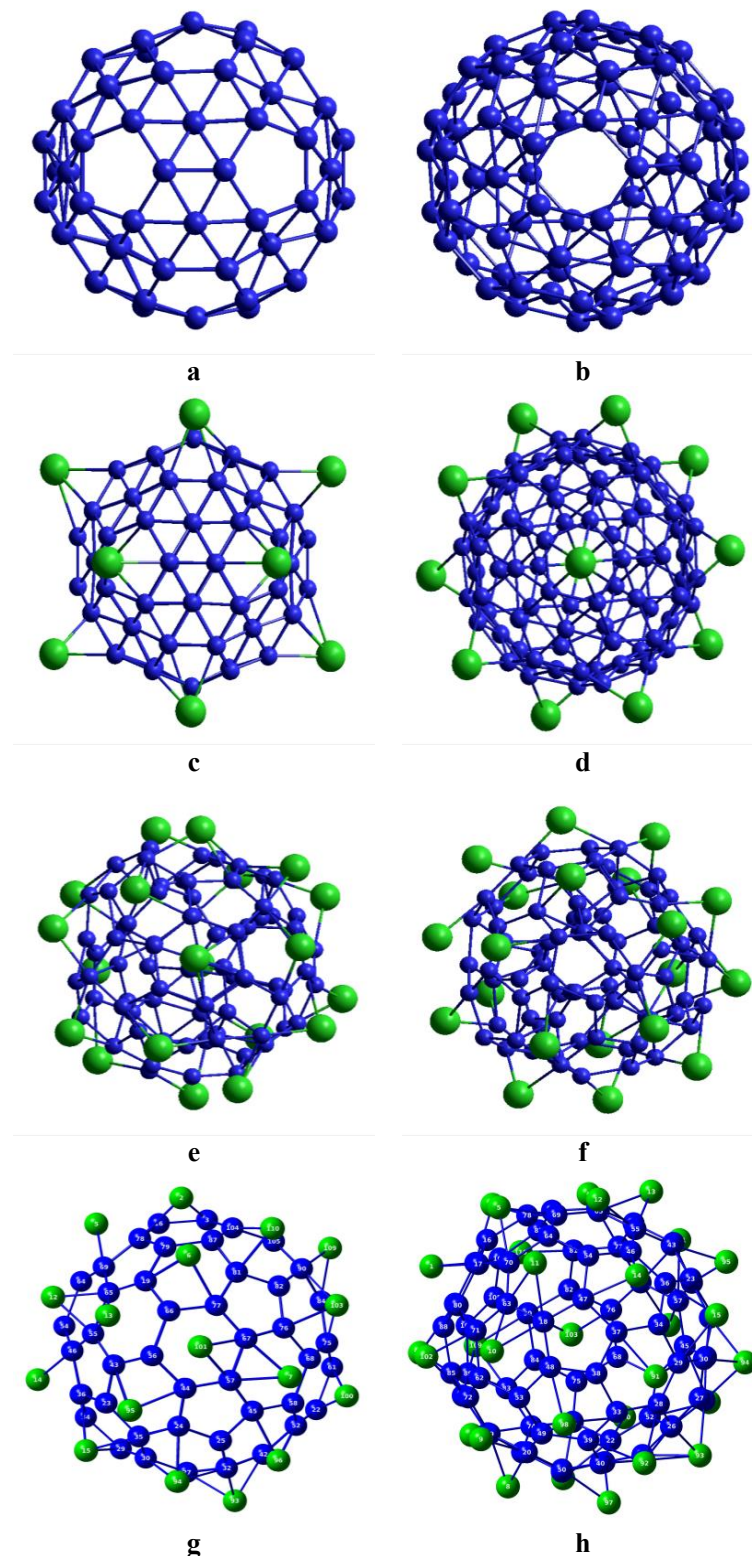


Fig. 1. Optimized configurations of side view of a) B₈₀, c) Mg₁₂B₈₀, e) Mg₂₀B₈₀ and g) Mg₃₀B₈₀. Optimized configurations of top view of b) B₈₀, d) Mg₁₂B₈₀, f) Mg₂₀B₈₀ and h) Mg₃₀B₈₀. The blue ball for B, the green ball for Mg.

Table 1. Mulliken charge distribution in the Mg and B atoms of the Mg₁₂B₈₀H₂ and average charge transfer (Δq) from Mg to B atoms in pentagonal faces of B₈₀ cage.

Mg atoms	B atoms in pentagonal faces of the B ₈₀ cage					Δq (e)
81(0.49)	10(-0.02)	42(-0.02)	43(-0.02)	57(-0.02)	59(-0.02)	0.59
82(0.49)	25(-0.01)	26(-0.02)	27(-0.02)	49(-0.02)	50(-0.02)	0.58
83(0.49)	5(-0.02)	6(-0.02)	15(-0.03)	16(-0.02)	17(-0.01)	0.59
84(0.49)	33(-0.01)	34(-0.02)	44(-0.02)	45(-0.02)	46(-0.02)	0.58
85(0.49)	20(-0.02)	21(-0.01)	54(-0.02)	55(-0.02)	56(-0.03)	0.59
86(0.49)	13(-0.02)	14(-0.03)	28(-0.02)	38(-0.02)	39(-0.01)	0.59
87(0.47)	31(-0.02)	32(-0.02)	40(-0.02)	41(-0.02)	58(-0.02)	0.57
88(0.47)	18(-0.02)	19(-0.02)	22(-0.02)	23(-0.02)	24(-0.02)	0.57
89(0.49)	47(-0.02)	48(-0.02)	51(-0.02)	52(-0.01)	53(-0.02)	0.58
90(0.49)	3(-0.03)	4(-0.02)	11(-0.02)	12(-0.02)	29(-0.01)	0.59
91(0.49)	30(-0.01)	35(-0.02)	36(-0.03)	37(-0.02)	60(-0.02)	0.59
92(0.49)	1(-0.02)	2(-0.03)	7(-0.01)	8(-0.02)	9(-0.02)	0.59

Table 2. Mulliken charge distribution in the Mg and B atoms of the Mg₂₀B₈₀H₂ and average charge transfer (Δq) from Mg to B atoms in hexagonal faces of the B₈₀ cage.

Mg atoms	B atoms in hexagonal faces of the B ₈₀ cage						Δq (e)
81(0.37)	32(-0.29)	33(-0.05)	41(-0.05)	42(-0.26)	43(-0.19)	44(-0.08)	1.29
82(0.40)	16(-0.10)	17(-0.15)	18(-0.12)	24(-0.18)	25(-0.00)	26(-0.09)	1.04
83(0.34)	7(-0.02)	8(-0.09)	19(-0.12)	20(-0.05)	21(-0.13)	22(-0.14)	0.89
84(0.30)	30(-0.08)	31(-0.05)	37(-0.10)	38(-0.07)	39(-0.12)	40(-0.11)	0.83
85(0.35)	8(-0.09)	9(-0.12)	10(-0.08)	20(-0.05)	56(-0.19)	68(-0.15)	1.03
86(0.33)	27(-0.08)	28(-0.12)	36(-0.12)	37(-0.10)	38(-0.07)	49(-0.11)	0.93
87(0.36)	21(-0.13)	22(-0.14)	23(-0.20)	52(-0.27)	53(-0.04)	54(-0.08)	1.22
88(0.42)	12(-0.00)	13(-0.14)	29(-0.09)	39(-0.12)	40(-0.11)	58(-0.14)	1.02
89(0.38)	23(-0.20)	24(-0.18)	25(-0.00)	50(-0.17)	51(-0.03)	52(-0.27)	1.23
90(0.37)	11(-0.04)	29(-0.09)	41(-0.05)	42(-0.26)	58(-0.14)	59(-0.20)	1.15
91(0.40)	1(-0.04)	6(-0.17)	7(-0.02)	17(-0.15)	18(-0.12)	19(-0.12)	1.02
92(0.32)	30(-0.08)	31(-0.05)	32(-0.29)	33(-0.05)	34(-0.14)	60(-0.11)	1.04
93(0.45)	1(-0.04)	2(-0.32)	3(-0.13)	4(-0.08)	5(-0.16)	6(-0.17)	1.35
94(0.39)	34(-0.14)	35(-0.12)	46(-0.06)	47(-0.09)	48(-0.17)	60(-0.11)	1.08
95(0.46)	43(-0.19)	44(-0.08)	45(-0.09)	55(-0.24)	56(-0.19)	68(-0.14)	1.39
96(0.42)	14(-0.05)	15(-0.22)	16(-0.10)	26(-0.09)	27(-0.08)	28(-0.12)	1.08
97(0.34)	45(-0.09)	46(-0.06)	47(-0.09)	53(-0.04)	54(-0.08)	55(-0.24)	0.94
98(0.32)	4(-0.08)	5(-0.16)	12(-0.00)	13(-0.14)	14(-0.05)	15(-0.22)	0.97
99(0.42)	35(-0.12)	36(-0.12)	48(-0.17)	49(-0.11)	50(-0.17)	51(-0.03)	1.14
100(0.40)	2(-0.32)	3(-0.13)	9(-0.12)	10(-0.08)	11(-0.04)	59(-0.20)	1.29

Table 3. Mulliken charge distribution in the Mg and B atoms of the Mg₃₀B₈₀H₂ and average charge transfer (Δq) from Mg to B atoms in hexagonal faces of the B₈₀ cage.

Mg atoms	B atoms in hexagonal faces of the B ₈₀ cage							Δq (e)
1(0.34)	3(-0.16)	16(-0.10)	17(-0.15)	80(-0.13)	88(-0.13)	107(-0.15)		1.16
2(0.34)	3(-0.16)	16(-0.10)	78(-0.16)	79(-0.12)	87(-0.15)	104(-0.13)		1.16
4(0.36)	60(-0.10)	73(-0.14)	74(-0.14)	83(-0.11)	86(-0.10)	89(-0.18)		1.13
5(0.36)	16(-0.10)	17(-0.15)	64(-0.09)	69(-0.12)	70(-0.12)	78(-0.16)		1.10
6(0.36)	19(-0.13)	66(-0.10)	77(-0.13)	79(-0.12)	81(-0.13)	87(-0.15)		1.11
7(0.33)	45(-0.15)	57(-0.16)	58(-0.10)	67(-0.16)	68(-0.10)	76(-0.15)		1.14
8(0.33)	20(-0.15)	21(-0.10)	50(-0.14)	59(-0.15)	60(-0.10)	73(-0.14)		1.12
9(0.33)	20(-0.15)	49(-0.12)	53(-0.09)	59(-0.15)	62(-0.09)	72(-0.12)		1.06
10(0.33)	18(-0.14)	48(-0.13)	53(-0.09)	62(-0.09)	63(-0.14)	71(-0.13)		1.04
11(0.33)	18(-0.14)	47(-0.12)	54(-0.09)	63(-0.14)	64(-0.09)	70(-0.12)		1.02
12(0.32)	46(-0.12)	54(-0.09)	55(-0.14)	64(-0.09)	65(-0.14)	69(-0.12)		1.01
13(0.33)	19(-0.13)	43(-0.13)	55(-0.14)	56(-0.10)	65(-0.14)	66(-0.10)		1.06
14(0.36)	34(-0.10)	36(-0.16)	37(-0.16)	46(-0.12)	47(-0.12)	54(-0.09)		1.11
15(0.34)	23(-0.12)	29(-0.16)	30(-0.13)	34(-0.10)	35(-0.15)	36(-0.16)		1.15
91(0.34)	28(-0.15)	29(-0.16)	33(-0.12)	34(-0.10)	37(-0.16)	38(-0.14)		1.17
92(0.35)	26(-0.11)	28(-0.15)	31(-0.18)	33(-0.12)	39(-0.15)	40(-0.10)		1.16
93(0.36)	26(-0.11)	27(-0.11)	31(-0.18)	32(-0.19)	41(-0.11)	42(-0.10)		1.17
94(0.35)	24(-0.13)	25(-0.10)	27(-0.11)	30(-0.13)	32(-0.19)	35(-0.15)		1.17
95(0.36)	23(-0.12)	24(-0.13)	35(-0.15)	43(-0.13)	44(-0.13)	56(-0.10)		1.11
96(0.36)	25(-0.10)	32(-0.19)	42(-0.10)	45(-0.15)	52(-0.14)	58(-0.10)		1.14
97(0.36)	21(-0.10)	31(-0.18)	40(-0.10)	41(-0.11)	50(-0.14)	51(-0.14)		1.13
98(0.36)	33(-0.12)	38(-0.14)	39(-0.15)	48(-0.13)	49(-0.12)	53(-0.09)		1.11
99(0.33)	21(-0.10)	22(-0.16)	51(-0.14)	60(-0.10)	61(-0.16)	74(-0.14)		1.13
100(0.33)	22(-0.16)	52(-0.14)	58(-0.10)	61(-0.16)	68(-0.10)	75(-0.14)		1.15
101(0.33)	44(-0.13)	56(-0.10)	57(-0.16)	66(-0.10)	67(-0.16)	77(-0.13)		1.09
102(0.36)	62(-0.09)	71(-0.13)	72(-0.12)	80(-0.13)	85(-0.15)	88(-0.13)		1.10
103(0.36)	68(-0.10)	75(-0.14)	76(-0.15)	82(-0.10)	84(-0.10)	90(-0.19)		1.14
108(0.35)	85(-0.15)	86(-0.10)	88(-0.13)	89(-0.18)	106(-0.11)	107(-0.15)		1.16
109(0.36)	83(-0.11)	84(-0.10)	89(-0.18)	90(-0.19)	105(-0.11)	106(-0.11)		1.17
110(0.35)	81(-0.13)	82(-0.10)	87(-0.15)	90(-0.19)	104(-0.13)	105(-0.11)		1.17

molecule and separate Mg atom, respectively, and m is the number of Mg atoms. The calculated binding energies are listed in Table 4. Our calculated results show that the average binding energy in the Mg₁₂B₈₀, Mg₂₀B₈₀ and Mg₃₀B₈₀ are -0.76, -1.13 and -0.35 eV/Mg, respectively. To investigate the interaction of the hydrogen

molecule with the B₈₀ coated with Mg, a hydrogen molecule is added to this system, that displaces the absorbed Mg atoms. The electric field due to the positively charged Mg atoms increases the polarizability of the H₂ molecule which leads to adsorption of H₂ molecule without dissociation.

The polarization interaction between the Mg

Table 4. Total energy (E), binding energies of Mg atoms on the B₈₀ (E_b) and adsorption energy (E_a) calculated using M062X/6-31G**//B3LYP/6-31G method, as well as H-H bond length in H₂ molecules.

	E (eV)	E _b (eV/Mg)	E _a (eV/H ₂)	H-H (Å)
Mg	-5443.29			
H ₂	-31.76		0.742	
B ₈₀	-54075.67			
B ₈₀ H ₂	-54107.45		-0.02	0.743
Mg ₁₂ B ₈₀	-119404.35	-0.76		
Mg ₁₂ B ₈₀ H ₂	-119436.33		-0.22	0.743
Mg ₂₀ B ₈₀	-162964.15	-1.13		
Mg ₂₀ B ₈₀ H ₂	-162995.97		-0.06	0.744
Mg ₃₀ B ₈₀	-217384.79	-0.35		
Mg ₃₀ B ₈₀ H ₂	-217416.61		-0.05	0.744

Table 5. Hydrogen absorption energy (E_a) on Metal-coated Boron nanostructures calculated in previous papers and this research.

Metal-coated Boron nanostructures	Ea(eV/H ₂)	Reference
B ₈₀	0.02	This research
Mg ₁₂ B ₈₀	0.22	This research
Mg ₂₀ B ₈₀	0.06	This research
Mg ₃₀ B ₈₀	0.05	This research
Na ₁₂ B ₈₀	0.07	[27]
K ₁₂ B ₈₀	0.09	[27]
Ca ₁₂ B ₈₀	0.12 - 0.40	[28]
Sc ₆ B ₄₀	0.33 - 0.58	[22]
Mg ₁₂ B ₈₀	0.20	[29]
Ti ₆ B ₄₀	0.20 - 0.40	[21]
Sc ₄ B ₃₈	0.22	[23]

atom and the absorbed H₂ molecule results in increase in the H-H bond length, compared to a single H₂ molecule, as can be seen in Table 4. Fig. 2 shows the adsorption of a H₂ molecule on B₈₀, Mg₁₂B₈₀ and Mg₃₀B₈₀ structures.

The hydrogen adsorption energy on boron fullerenes doped with magnesium is calculated by:

$$E_a = (E_{MgB_{80}H_2} - E_{MgB_{80}} - nE_{H_2})/n \quad (2)$$

where E_{MgB₈₀H₂}, E_{MgB₈₀} and E_{H₂} are the energy of H₂ on B₈₀ doped with magnesium, the energy of B₈₀ doped with magnesium and the energy of H₂ molecule, respectively, and n reflects the number of adsorbed H₂ molecules. Total energies of the structures and adsorption energies per H₂ molecule as well as H-H bond lengths in H₂ molecules are given in Table 4. Entries in table 4 shows that boron fullerenes doped with magnesium atoms

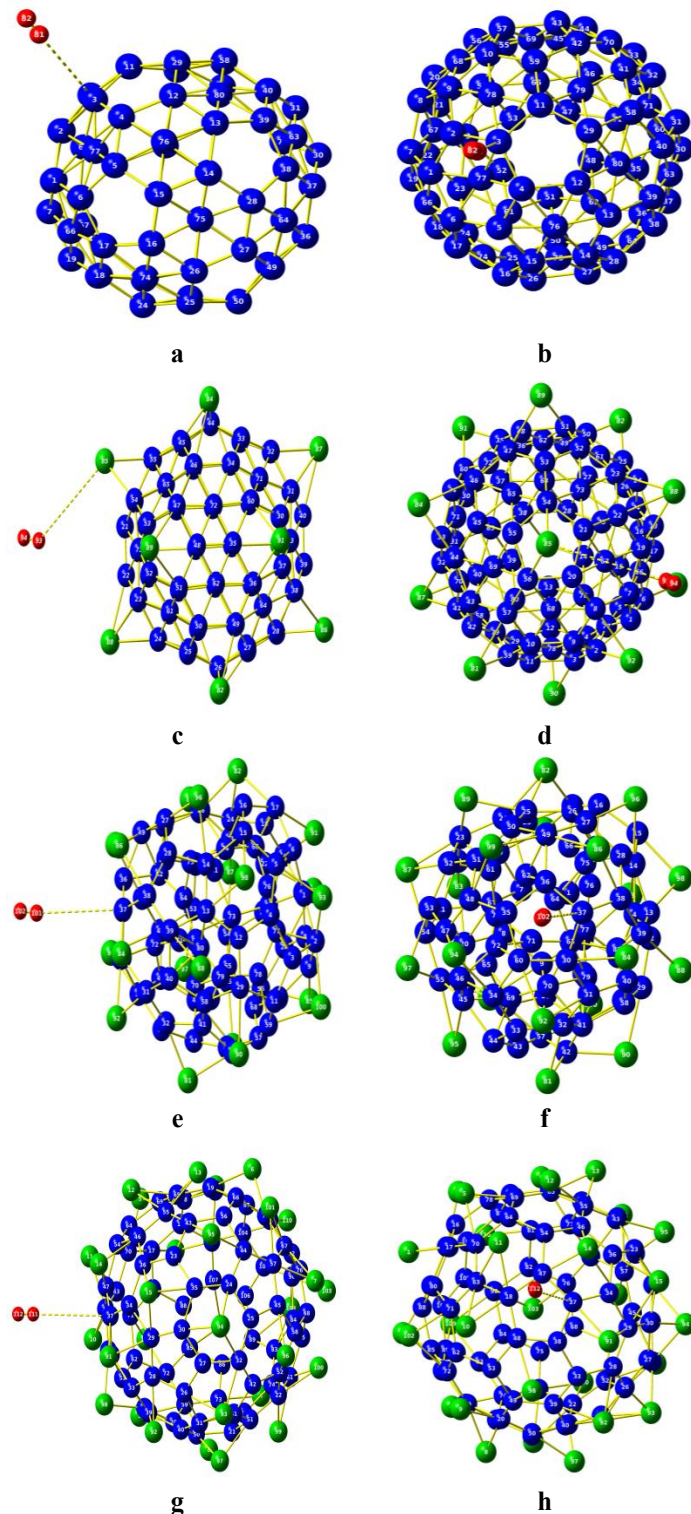


Fig. 2. Side view of optimized configurations of one H_2 molecule adsorbed on a) B_{80} , c) $Mg_{12}B_{80}$, e) $Mg_{20}B_{80}$, g) $Mg_{30}B_{80}$ along with the number of atoms. Top view of the optimized configurations of one H_2 molecule adsorbed on b) B_{80} , d) $Mg_{12}B_{80}$, f) $Mg_{20}B_{80}$, and h) $Mg_{30}B_{80}$. The blue ball for B, the green ball for Mg, and the red ball for H

Table 6. $\rho(r)$, $\nabla^2\rho$, $G(r)$, $K(r)$ and $V(r)$, (in atomic units) for the critical point between bonds in B₈₀H₂ molecule

Bond	$\rho(r)$	$G(r)$	$K(r)$	$\nabla^2(\rho)$	$V(r)$
H(81)-H(82)	0.2690	0.00003	0.3410	-1.3637	0.3410
H(81)-B(3)	0.0024	0.0012	-0.0004	0.0065	0.0008
B(3)-B(2)	0.1394	0.0475	0.0914	-1.1754	0.1389
B(3)-B(4)	0.1342	0.0360	0.847	-0.1950	0.1207
B(3)-B(11)	0.1253	0.0314	0.0703	-0.1556	0.1017
B(3)-B(77)	0.1223	0.0507	0.0724	-0.0868	0.1232
B(3)-B(78)	0.1196	0.0475	0.0683	-0.0832	0.1158

Table 7. $\rho(r)$, $\nabla^2\rho$, $G(r)$, $K(r)$ and $V(r)$, (in atomic units) for the critical point between bonds in Mg₁₂B₈₀H₂ molecule

Bond	$\rho(r)$	$G(r)$	$K(r)$	$\nabla^2(\rho)$	$V(r)$
H(93)-H(94)	0.2465	0.00001	0.2660	-1.0642	0.2661
H(94)-Mg(85)	0.0003	0.0001	-0.00005	0.0006	0.00005
Mg(85)-B(54)	0.0264	0.0259	-0.0008	0.1066	0.0251
Mg(85)-B(55)	0.0254	0.0251	-0.0001	0.1043	0.0241
Mg(85)-B(56)	0.0259	0.0256	-0.0001	0.1059	0.0247

Table 8. $\rho(r)$, $\nabla^2\rho$, $G(r)$, $K(r)$ and $V(r)$, (in atomic units) for the critical point between bonds in Mg₂₀B₈₀H₂ molecule

Bond	$\rho(r)$	$G(r)$	$K(r)$	$\nabla^2(\rho)$	$V(r)$
H(101)-H(102)	0.2457	0.0001	0.2643	-1.0568	0.2643
H(101)-B(37)	0.0011	0.0005	-0.0002	0.0028	0.0003
B(37)-B(30)	0.1305	0.0209	0.0742	-0.2130	0.0951
B(37)-B(36)	0.1305	0.0216	0.0751	-0.2138	0.0967
B(37)-B(38)	0.1214	0.0222	0.0646	-0.1696	0.0868

have more hydrogen absorption capacity than boron fullerenes. The adsorption energies for B₈₀, Mg₁₂B₈₀, Mg₂₀B₈₀ and Mg₃₀B₈₀ are -0.02, -0.22, -0.06 and -0.05 eV/H₂, respectively. Mg₁₂B₈₀ has the highest adsorption energy, which indicates that its reactivity and hydrogen storage capability is more than B₈₀, Mg₂₀B₈₀ and Mg₃₀B₈₀, which corresponds to the condition of the reversible hydrogen molecular absorption (between 0.2 and 0.4 eV/H₂). Table 5 includes a comparison of the results of

our calculations and the calculations of previous papers for the values of hydrogen absorption energy on Metal-coated Boron nanostructures.

To determine the type of interaction of hydrogen molecule with B₈₀, Mg₁₂B₈₀, Mg₂₀B₈₀ and Mg₃₀B₈₀, critical points of electron density distribution have been calculated by using AIM2000 software. The results of these calculations, such as the values of charge density, $\rho(r)$, Laplacian of ρ , $\nabla^2(\rho)$, Lagrangian Kinetic Energy, $G(r)$, Hamiltonian

Table 9. ρ(r), ∇²ρ, G(r), K(r) and V(r), (in atomic units) for the critical point between bonds in Mg₃₀B₈₀H₂ molecule

bond	ρ(r)	G(r)	K(r)	∇ ² (ρ)	V(r)
H(111)-H(112)	0.0290	0.00005	0.3400	-1.36	0.3400
H(112)-B(37)	0.0013	0.0005	-0.0002	0.0029	0.0003
B(37)-B(34)	0.1280	0.0217	0.0759	-0.2170	0.0976
B(37)-B(38)	0.1350	0.0190	0.0828	-0.2550	0.1020
B(37)-B(47)	0.1410	0.0217	0.0906	-0.2760	0.1120

Table 10. Some electronic properties of B₈₀, B₈₀H₂, Mg₁₂B₈₀, Mg₁₂B₈₀H₂, Mg₂₀B₈₀, Mg₂₀B₈₀H₂, Mg₃₀B₈₀ and Mg₃₀B₈₀H₂ structures in eV

Molecule	E _H	E _L	ΔE _{H-L}	χ	η	IP	EA
B ₈₀	-5.34	-3.58	1.76	4.46	0.88	5.34	3.58
B ₈₀ H ₂	-5.35	-3.58	1.77	4.47	0.89	5.35	3.58
Mg ₁₂ B ₈₀	-3.77	-3.14	0.63	3.45	0.32	3.77	3.14
Mg ₁₂ B ₈₀ H ₂	-3.83	-3.27	0.56	3.55	0.28	3.83	3.27
Mg ₂₀ B ₈₀	-2.98	-2.24	0.74	2.61	0.37	2.98	2.24
Mg ₂₀ B ₈₀ H ₂	-2.99	-2.24	0.75	2.62	0.38	2.99	2.24
Mg ₃₀ B ₈₀	-2.90	-2.23	0.67	2.56	0.33	2.90	2.23
Mg ₃₀ B ₈₀ H ₂	-2.91	-2.23	0.68	2.57	0.34	2.91	2.23

Kinetic Energy, K(r), and Virial Field Function, V(r), for the hydrogen absorption bond and the corresponding atoms, have been shown in Tables 6 to 9. Our calculated results show that the ∇²(ρ) values, for the critical points between the hydrogen molecule and B₈₀, Mg₁₂B₈₀, Mg₂₀B₈₀ and Mg₃₀B₈₀, are all positive and consequently of electrostatic type.

The ∇²(ρ) value for Mg₁₂B₈₀ is lower than that B₈₀, Mg₂₀B₈₀ and Mg₃₀B₈₀, which is equal to 0.0006, 0.0065, 0.0028 and 0.0029, respectively. By plotting the molecular graph, we found that the critical point of H₂ molecule adsorption on Mg₁₂B₈₀ is located between the H atom and the Mg atoms on the pentagonal boron ring, while the critical point of H₂ molecule adsorption on Mg₂₀B₈₀ and Mg₃₀B₈₀ is located between the H and one of the B atoms in the hexagonal boron ring.

By using the energy of HOMO and LUMO

orbitals, E_H and E_L, the values of ionization energy (IP), electron affinity (EA), electronegativity (χ), and hardness (η) can be obtained:

$$IP \approx -E_H, EA \approx -E_L, \eta = (IP - EA)/2, \chi = (IP + EA)/2 \quad (3)$$

Some electronic properties of B₈₀, B₈₀H₂, Mg₁₂B₈₀, Mg₁₂B₈₀H₂, Mg₂₀B₈₀, Mg₂₀B₈₀H₂, Mg₃₀B₈₀ and Mg₃₀B₈₀H₂ are given in Table 10.

Table 10 shows Mg₁₂B₈₀ possesses the lowest value of ΔE_{H-L} which indicates a lower kinetic stability (higher reactivity) of this structure compared to B₈₀, Mg₂₀B₈₀ and Mg₃₀B₈₀. When a hydrogen molecule binds to these structures, the ΔE_{H-L} increases which indicates that the adsorption potency decreases for subsequent hydrogen molecule. Also, the hardness value (η) for Mg₁₂B₈₀ is lower than for B₈₀, Mg₂₀B₈₀ and Mg₃₀B₈₀ which shows that it has a lower energy

Table 11. Molecular descriptors for B₈₀, Mg₁₂B₈₀, Mg₂₀B₈₀ and Mg₃₀B₈₀

descriptors	B ₈₀	Mg ₁₂ B ₈₀	Mg ₂₀ B ₈₀	Mg ₃₀ B ₈₀	Definition of descriptors
V index	0.12	0.11	0.10	0.08	Balaban V index
X index	0.16	0.15	0.14	0.11	Balaban X index
Y index	0.46	0.44	0.39	0.28	Balaban Y index
ZM1	2220	2640	1440	1350	first Zagreb index
ZM2	5850	7215	2792	1470	second Zagreb index
BBI	900	1080	539	490	Bertz branching index
DBI	23.66	26.31	16.29	14.63	Dragon branching index
Pol	540	685	749	636	polarity number
MSD	4.55	4.68	4.89	6.14	mean square distance index (Balaban)
VAR	8	54	194	84	Variation
SMTI	1.45×10 ⁵	1.95×10 ⁵	1.65×10 ⁵	2.30×10 ⁵	Schultz Molecular Topological Index
Wap	3.94×10 ⁷	6.93×10 ⁸	1.84×10 ⁷	6.11×10 ⁶	all-path Wiener index
PHI	0.12	0.2	2.38	5.23	Kier flexibility index
DELS	20.57	40.98	79.42	73.22	molecular electro topological variation
TIE	145.30	183	180	181.8	E-state topological parameter
MLOGP	-1.43	-1.43	-1.43	-1.43	Moriguchi octanol-water partition coeff. (logP)
MLOGP2	2.05	2.05	2.05	2.05	squared Moriguchi octanol-water partition coeff. (logP ²)
VvdwMG	62.74	180	612.4	802.4	van der Waals volume from McGowan volume

gap and more reactivity. Numerical value of some molecular descriptors for B₈₀, Mg₁₂B₈₀, Mg₂₀B₈₀ and Mg₃₀B₈₀ which were calculated using Dragon ver. 7 (5270/3D) has been given in Table 11.

The data show that values of MLOGP and MLOGP2 for B₈₀, Mg₁₂B₈₀, Mg₂₀B₈₀ and Mg₃₀B₈₀ are the same, the values of ZM1, ZM2, DBI, BBI, TIE and Wap for Mg₁₂B₈₀ are higher than B₈₀, Mg₂₀B₈₀ and Mg₃₀B₈₀. Also, the values of VvdwMG, PHI and MSD increases according to the number of atoms and the size of the structure, while values of V index, X index and Y indices decreases with respect to the number of atoms and the size of the structure. In other words, values of these descriptors depends on the size and number of atoms in the structure. Therefore, it can be concluded higher values of

ZM1, ZM2, DBI, BBI, TIE and Wap, result in higher adsorption capability.

CONCLUSION

Through B3LYP/6-31G//M062X/6-31G** calculations, results showed that magnesium doping of boron fullerenes rises the hydrogen storage capacity. Mg atoms binds to the boron fullerenes due to the charge transfer from Mg to B atoms. This charge transfer creates an electric field around Mg atoms with a positive charge when hydrogen molecules approach the system, the hydrogen molecules become polarized, and they are adsorbed to these boron fullerenes doped with Mg atoms. Analysis of critical points shows that the Laplacian of ρ , $\nabla^2(\rho)$, for the critical

points between the hydrogen molecule and B₈₀, Mg₁₂B₈₀, Mg₂₀B₈₀ and Mg₃₀B₈₀ is a positive value, revealing an electrostatic interaction. Our results show that Mg₁₂B₈₀ possesses the lowest ΔE_{H-L} and the highest adsorption energy, which indicates higher reactivity of this structure compared to B₈₀, Mg₂₀B₈₀ and Mg₃₀B₈₀. Also, the hardness value (η) for Mg₁₂B₈₀ is lower than those of B₈₀, Mg₂₀B₈₀ and Mg₃₀B₈₀, that shows a lower energy gap and more reactivity. Numerical values of some molecular descriptors show that for Mg₁₂B₈₀, values of ZM1, ZM2, DBI, BBI, TIE and Wap are all higher than other structures, that results higher adsorption capacity.

CONFLICT OF INTEREST

The authors declare that there is no conflict of interests regarding the publication of this manuscript.

REFERENCES

- Zhang Z, Zheng W, Jiang Q. Hydrogen adsorption on Ce/SWCNT systems: a DFT study. *Physical Chemistry Chemical Physics*. 2011;13(20):9483-9489.
- Xia Y, Yang Z, Zhu Y. Porous carbon-based materials for hydrogen storage: advancement and challenges. *Journal of Materials Chemistry A*. 2013;1(33):9365-9381.
- Xia Y, Walker GS, Grant DM, Mokaya R. Hydrogen storage in high surface area carbons: experimental demonstration of the effects of nitrogen doping. *Journal of the American Chemical Society*. 2009;131(45):16493-16499.
- Wu X, Gao Y, Zeng XC. Hydrogen storage in pillared Li-dispersed boron carbide nanotubes. *The Journal of Physical Chemistry C*. 2008;112(22):8458-8463.
- Wang Q, Sun Q, Jena P, Kawazoe Y. Theoretical study of hydrogen storage in Ca-coated fullerenes. *Journal of chemical theory and computation*. 2009;5(2):374-379.
- Umegaki T, Yan J-M, Zhang X-B, Shioyama H, Kuriyama N, Xu Q. Boron-and nitrogen-based chemical hydrogen storage materials. *International Journal of Hydrogen Energy*. 2009;34(5):2303-2311.
- Seenithurai S, Pandyan RK, Kumar SV, Saranya C, Mahendran M. Li-decorated double vacancy graphene for hydrogen storage application: a first principles study. *international journal of hydrogen energy*. 2014;39(21):11016-11026.
- Pupysheva OV, Farajian AA, Yakobson BI. Fullerene nanocage capacity for hydrogen storage. *Nano Letters*. 2008;8(3):767-774.
- Mananghaya MR. Hydrogen saturation limit of Ti-doped BN nanotube with BN defects: An insight from DFT calculations. *international journal of hydrogen energy*. 2018;43(22):10368-10375.
- Liu C, Fan Y, Liu M, Cong H, Cheng H, Dresselhaus MS. Hydrogen storage in single-walled carbon nanotubes at room temperature. *Science*. 1999;286(5442):1127-1129.
- Gayathri V, Devi N, Geetha R. Hydrogen storage in coiled carbon nanotubes. *International Journal of Hydrogen Energy*. 2010;35(3):1313-1320.
- Dillon AC, Jones K, Bekkedahl T, Kiang C, Bethune D, Heben M. Storage of hydrogen in single-walled carbon nanotubes. *Nature*. 1997;386(6623):377-379.
- Broom DP, Hirscher M. Irreproducibility in hydrogen storage material research. *Energy & Environmental Science*. 2016;9(11):3368-3380.
- Zimmermann U, Malinowski N, Burkhardt A, Martin T. Metal-coated fullerenes. *Carbon*. 1995;33(7):995-1006.
- Pederson M, Porezag D, Patton D, Kaxiras E. Metal-coated fullerenes: electronic, geometrical and vibrational properties of C60M62 (M= Ti and V). *Chemical physics letters*. 1999;303(3-4):373-378.
- Nakajima A, Nagao S, Takeda H, Kurikawa T, Kaya K. Multiple dumbbell structures of vanadium-C60 clusters. *The Journal of chemical physics*. 1997;107(16):6491-6494.
- Nagao S, Kurikawa T, Miyajima K, Nakajima A, Kaya K. Formation and Structures of Transition Metal-C60 Clusters. *The Journal of Physical Chemistry A*. 1998;102(24):4495-4500.
- Balch AL, Olmstead MM. Reactions of transition metal complexes with fullerenes (C60, C70, etc.) and related materials. *Chemical reviews*. 1998;98(6):2123-2166.
- Rayane D, Antoine R, Dugourd P, Benichou E, Allouche A-R, Aubert-Frécon M, et al. Polarizability of KC60: evidence for potassium skating on the C60 surface. *Physical review letters*. 2000;84(9):1962.
- Kubas GJ. Metal-dihydrogen and σ-bond coordination: the consummate extension of the Dewar-Chatt-Duncanson model for metal-olefin π bonding. *Journal of Organometallic Chemistry*. 2001;635(1-2):37-68.
- Dong H, Hou T, Lee S-T, Li Y. New Ti-decorated B40 fullerene as a promising hydrogen storage material. *Scientific reports*. 2015;5(1):9952.
- Tang C, Zhang X. The hydrogen storage capacity of Sc atoms decorated porous boron fullerene B40: a DFT study. *International Journal of Hydrogen Energy*. 2016;41(38):16992-16999.
- Liu P, Liu F, Wang Q, Ma Q. DFT simulation on hydrogen storage property over Sc decorated B38 fullerene. *International Journal of Hydrogen Energy*. 2018;43(42):19540-19546.
- Zhao Y, Lusk MT, Dillon AC, Heben MJ, Zhang SB. Boron-based organometallic nanostructures: hydrogen storage properties and structure stability. *Nano letters*. 2008;8(1):157-161.
- Wu W, Tian Z, Dong S. Yttrium-dispersed B80 fullerenes: promising materials for hydrogen storage. *Europhysics Letters*. 2015;109(5):56004.
- Wu G, Wang J, Zhang X, Zhu L. Hydrogen storage on metal-coated B80 buckyballs with density functional theory. *The Journal of Physical Chemistry C*. 2009;113(17):7052-7057.
- Li Y, Zhou G, Li J, Gu B-L, Duan W. Alkali-metal-doped B80 as high-capacity hydrogen storage media. *The Journal of Physical Chemistry C*. 2008;112(49):19268-19271.
- Li M, Li Y, Zhou Z, Shen P, Chen Z. Ca-coated boron fullerenes and nanotubes as superior hydrogen storage materials. *Nano letters*. 2009;9(5):1944-1948.
- Li J, Hu Z, Yang G. High-capacity hydrogen storage of magnesium-decorated boron fullerene. *Chemical Physics*. 2012;392(1):16-20.
- Cabria I, López M, Alonso J. Density functional calculations of hydrogen adsorption on boron nanotubes and boron sheets. *Nanotechnology*. 2006;17(3):778.
- Szwacki NG, Sadrzadeh A, Yakobson BI. B80 fullerene: an

- ab initio prediction of geometry, stability, and electronic structure. *Physical review letters.* 2007;98(16):166804.
32. Kim G, Jhi S-H. Ca-decorated graphene-based three-dimensional structures for high-capacity hydrogen storage. *The Journal of Physical Chemistry C.* 2009;113(47):20499-20503.
33. Yoon M, Yang S, Hicke C, Wang E, Geohegan D, Zhang Z. Calcium as the superior coating metal in functionalization of carbon fullerenes for high-capacity hydrogen storage. *Physical review letters.* 2008;100(20):206806.
34. Zhao Y, Kim Y-H, Dillon A, Heben M, Zhang S. Hydrogen storage in novel organometallic buckyballs. *Physical review letters.* 2005;94(15):155504.
35. Rabilloud F, Antoine R, Broyer M, Compagnon I, Dugourd P, Rayane D, et al. Electric dipoles and susceptibilities of alkali clusters/fullerene complexes: experiments and simulations. *The Journal of Physical Chemistry C.* 2007;111(48):17795-17803.
36. Frisch M, Trucks G, Schlegel H, Scuseria G, Robb M, Cheeseman J, et al. Gaussian 09, Revision D. 01, Gaussian, Inc., Wallingford CT. See also: URL: <http://www.gaussian.com>. 2009.
37. Kohn W, Sham LJ. Self-consistent equations including exchange and correlation effects. *Physical review.* 1965;140(4A):A1133.
38. König FB, Schönbohm J, Bayles D. AIM2000-a program to analyze and visualize atoms in molecules. *Journal of Computational Chemistry.* 2001;22(5):545-559.
39. Mauri A, Consonni V, Pavan M, Todeschini R. Dragon software: An easy approach to molecular descriptor calculations. *Match.* 2006;56(2):237-248.